International Journal of Environment and Geoinformatics (IJEGEO) is an international, multidisciplinary, peer reviewed and open access journal.

Determining Roughness Angle of Limestone Using Optical Laser Scanner

E. Özgür Avşar, Erkan Bozkutoğlu, Umut Aydar, Dursun Zafer Şeker, Şinasi Kaya and Cem Gazioğlu[3]

Editors

Prof. Dr. Cem Gazioğlu, Prof. Dr. Dursun Zafer Şeker, Prof. Dr. Ayşegül Tanık, Assoc. Prof. Dr. Şinasi Kaya

Scientific Committee

Assoc. Prof. Dr. Hasan Abdullah (BL), Assist. Prof. Dr. Alias Abdulrahman (MAL), Assist. Prof. Dr. Abdullah Aksu, (TR); Assist. Prof. Dr. Sinan S. Arkın (TR), Prof. Dr. Hasan Atar (TR), Prof. Dr. Lale Balas (TR), Prof. Dr. Levent Bat (TR), Assoc. Prof. Dr. Füsun Balık Şanlı (TR), Prof. Dr. Nuray Balkıs Çağlar (TR), Prof. Dr. Bülent Bayram (TR), Prof. Dr. Şükrü Turan Beşiktepe (TR), Prof. Dr. Z. Selmin (TR), Assoc. Prof. Dr. Gürcan Büyüksalih (TR), Dr. Jadunandan Dash (UK), Assist. Prof. Dr. Volkan Demir (TR), Assoc. Prof. Dr. Hande Demirel (TR), Assoc. Prof. Dr. Nazlı Demirel (TR), Dr. Arta Dilo (NL), Prof. Dr. A. Evren Erginal (TR), Assoc. Prof. Dr. Murat Gündüz (TR), Assoc. Prof. Dr. Kensuke Kawamura (JAPAN), Prof. Dr. Fatmagül Kılıç (TR), Prof. Dr. Ufuk Kocabaş (TR), Prof. Dr. Yusuf Kurucu (TR), Prof. Dr. Hakan Kutoğlu (TR), Prof. Dr. Nebiye Musaoğlu (TR), Prof. Dr. Erhan Mutlu (TR), Assist. Prof. Dr. Hakan Öniz (TR), Assoc. Prof. Dr. Hasan Özdemir (TR), Assoc. Prof. Dr. Barış Salihoğlu (TR), Prof. Dr. Elif Serter (TR), Prof. Dr. Kadir Seyhan (TR), Prof. Dr. Murat Sezgin (TR), Prof. Dr. Nüket Sivri (TR), Assoc. Prof. Dr. Uğur Şanlı (TR), Assoc. Prof. Dr. Seyfettin Taş (TR), Assoc. Prof. Dr. İ. Noyan Yılmaz (TR), Assist. Prof. Dr. Baki Yokeş (TR), Assist. Prof. Dr. Sibel Zeki (TR), Dr. Hakan Kaya (TR).

Determining Roughness Angle of Limestone Using Optical Laser Scanner

E. Özgür Avşar[1,*], Erkan Bozkutoğlu[2], Umut Aydar[2], Dursun Zafer Şeker[2], Şinasi Kaya[2] and Cem Gazioğlu[3]

[1] Çanakkale Onsekiz Mart University, Engineering Faculty, Department of Geomatic Engineering 17100 Çanakkale TR
[2] ITÜ, Civil Engineering Faculty, Department of Geomatic Engineering, 34469 Maslak İstanbul TR
[3] Istanbul University, Institute of Marine Sciences and Management, Department of Marine Environment, 34134 Vefa Fatih Istanbul TR

Corresponding author.
Tel: +90 (286) 218 05 40

Received 15 November 2016
Accepted 01 December 2016

Abstract

In this study, a limestone rock core specimen with 6.94 cm x 4.95 cm dimensions was exposed to tensile force by Brazilian test and rough surfaces were obtained. Following the Brazilian test, roughness angles were measured by a laser scanner along one side of the rock specimen. For this purpose, Nextengine 3D Desktop scanner was used. The 17 profiles were studied along the width of the core with a 0.3 mm interval. Approximately 10000 points produced for each profile, some of them are in the "+" and some are in the "-" direction along each profile. Maximum and minimum roughness angles are calculated as 65.580 and 1.56x10-5 degree respectively. The average roughness angle value of the profiles is 13.870. The percentage of the roughness angle between 13 and 14 degrees were 2.65% and 2.70% for "-" and "+" directions on the rock surface, respectively. Mathematical analyses of 17 profiles showed that roughness profiles can be expressed by 21st – 30th degree polynomial equations with approximately 10-4 degree standard deviation.

Keywords: Roughness angle, limestone, image processing, surface roughness forecast

Introduction

Surface geometry of a rock is important for several reasons. The specification of shear strength parameters for discontinuous surfaces that is related to roughness angle is of fundamental concern to engineers charging with designing rock slopes or rock foundations for heavy structures (Jaeger, 1971). Rocks have 3 factors considered as surface characteristics of discontinuities. These are namely the waviness or undulation of the surface that results in variations in orientation or attitude along a given discontinuity; the smaller scale roughness of the surface that provides friction between two adjacent blocks; and the physical properties of any material that may fill the space between the two bounding surfaces of a discontinuity. When any shear failure takes place along a continuous joint surface; the surface roughnesses bear an important role on the shear strength of the intact rock. Waviness and roughness of rock surfaces were originally defined by Patton (1966) as first- and second-order irregularities based on their relative magnitudes. A series of 2nd order, generally more steeply inclined, undulations is superimposed on larger, more shallowly inclined 1st order undulations. Furthermore, 2nd order undulation, namely the roughness, governs an important role on shearing with a low normal stress until they are crushed and the 1st order undulation which is the waviness of the discontinuity takes a major role on sliding. Due to this fact, determining the undulations of

discontinuity is important and for the calculation of the peak shear strength. There are several ways of obtaining surface characteristics of discontinuities using relevant techniques; such as mechanical profiling (Fecker and Rengers, 1971; ISRM, 1978; Weissbach, 1978), compass and disc-clinometer (Fecker and Rengers, 1971), straight edge (Milne et al., 1991), shadow profilometry (Maerz et al., 1990), and tangent plane and connected pin sampling (Harrison and Rasouli, 2001). Recently, joint roughness can be measured precisely using non-contact methods like photogrammetry (Wickens and Barton, 1971; ISRM, 1978), image processing (Galante et al., 1991), fiber optic probe, He-Ne laser beam (Yılbas and Hasmi, 1999), interferometry topometric sensor (Grasselli and Egger, 2000), laser scanning (Fardin et al., 2004; Hong et al., 2006; Rahman et al., 2006), and electronic stylus profilometers (Grima, 1994; Kerstiens, 1999). Optical means of profiling uses light beams to measure undulation and roughness of a profile without giving any damages to the surface and asperities. This method contains interferometry, speckle metrology and laser profilometry. In this study, the main goal is determining the minimum, average and maximum roughness angle (i) of Class 2 limestone, according to the Anon (1979) classification.

In this study, the roughness surface was created from a Class 2 limestone rock core specimen with 6.94 cm x 4.95 cm dimensions after the Brazilian test. The roughness angles were measured from the surface of one part of limestone core specimen following the Brazilian test using Nextengine 3D Desktop scanner. It is a low-cost scanner which provides precise 3D point cloud. After modelling of the surface; the roughness profiles were detected at 0.3 mm interval and roughness angles were obtained from 17 cross- sections with approximately 10000 points for each profile. The roughness angles of the core specimen are 65.58 degree for maximum and 1.56x10-5 degree for minimum value which cannot be calculated using conventional techniques. The average roughness value of the 17 roughness profiles were calculated as 13.87 degrees.

Method

Measuring the Roughness Profiles Using Optical Laser Scanner

In recent years, by the rapid development of computer technology, graphic processors of personal computers have been strengthened and thus, the use of 3D modelling has accelerated in both scientific arena and among the end users. Together with the increasing demand to 3D models, high cost of the commercial laser scanners and the difficulty of processing the data from these devices have led to the development of low-cost 3D laser scanning systems (Aydar et al., 2011). The main principle of optical scanners is triangulation. According to the triangulation principle, it is possible to calculate the 3D object coordinate "C" if the distance "d" between the camera (B) and the laser source (A) and two angles "α", "β" of triangle are known (Fig. 1). Magnitude of "γ" angle affects the depth resolution. Depth resolution increases parallel to the increment of the angles (Zagorchev and Goshtasby, 2006).

In this study, Nextengine 3D Desktop scanner was used (Fig. 2). Nextengine 3D desktop scanner is a low-cost scanner which provides precise 3D point cloud fast. Accuracy of the system is specified by the manufacturer as ±0.127 mm for macro mode and ±0.328 mm for wide mode. According to the technical specs of the scanner, there is no pre-set limit for the object size. Objects, larger than the field of view of the scanner can be composite-captured with supplied software. For larger objects, scanner can be used as mounted on a tripod and it is possible to make partial scans by choosing the single scan mode. Used scanner provides 5.1" x 3.8" field size in Macro and 13.5" x 10.1" in Wide mode.

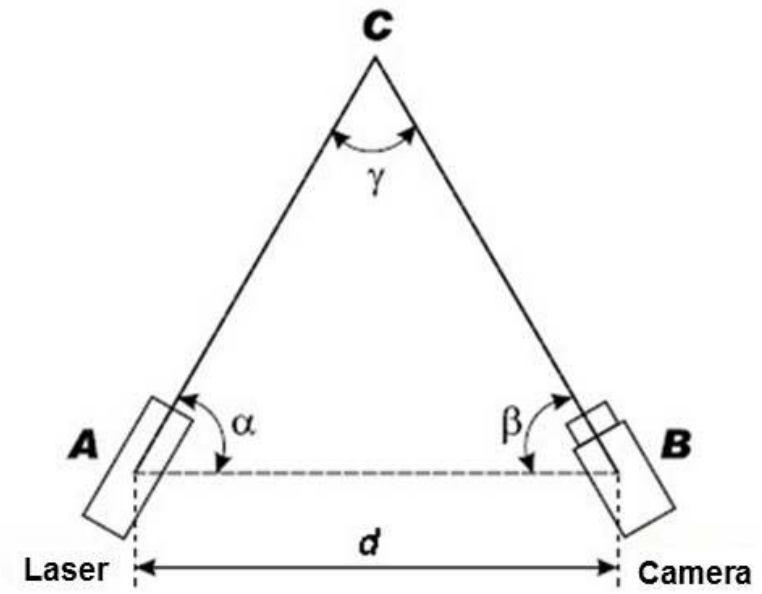

Figure 1Triangulation method in 3D Scanning.

Data Acquisition and Processing

The roughness surface was created with a 1.091 Mpa tensile force. The dry unit weight values change between 1.954 Mg/m3 and 1.997 Mg/m3, and the porosity values change between 18% and 20%. According to Anon (1979) classification, the Class 2 rocks has a "low density" and "high porosity", and the limit values vary between 1.8 and 2.2 Mg/m3 for the dry density and 30 – 15% for the porosity.

To determine the roughness angle of the limestone; rock sample was placed on the rotating tray which was about 15 cm away from the scanner. It is important that the whole object should be placed in the view of the camera of the scanner. ScanStudio HD software is used during the scanning and evaluation process. The tray has the capability of rotating the object 360o and predefined angles. The alignment of the point clouds are done automatically by the same software. The position of both the scanner and the object should not be changed during the scanning process to carry out the automatic alignment process. At the end of the scanning, 3D model of the rock pieces were obtained and saved with a ".vrl" extension and exported to Geomagic Studio software to further conduct some necessary filtering process. A low-level noise reduction was applied to the model and then, a number of points were reduced by applying curvature sample method. Curvature sample method preserves the details by reducing the number of points at flat areas while preserving the number of points at non-flat parts (Akça et al., 2007). After the post-processing steps, mesh model was generated from point cloud. The final model still contains some occluded areas due to the view angle and lack of the light during scanning. These areas should be filled by selecting the appropriate interpolation method of the software. Since the roughness of the surfaces is of concern in this study, curvature-based method was chosen to preserve the curves. After getting the full 3D object model, cross-sections on the surface are taken with approximately ~0.3 mm intervals in order to obtain the breaking angles (Fig. 3).



Figure 2. 3D Desktop Scanner and Object.

Curvature based method preserves the details by reducing the point number at flat areas while preserving the number of points at non-flat parts (Akça et al., 2007). This method specifies whether the fill process inserts flat or almost flat polygons into the hole, or attempts to match the surrounding curvature. After post-processing steps, mesh model was generated from point cloud. The final model still had some occluded areas due to the viewing angle and lack of the light during the scanning. These occluded areas should be filled by choosing the appropriate interpolation method of the software. Since the roughnesses of the surfaces are matters in this study, curvature-based method was chosen in order to preserve the curves. After getting the full 3D object model, cross-sections on the surface are taken with approximately 2 mm interval in order to obtain the breaking angles (Fig. 3).

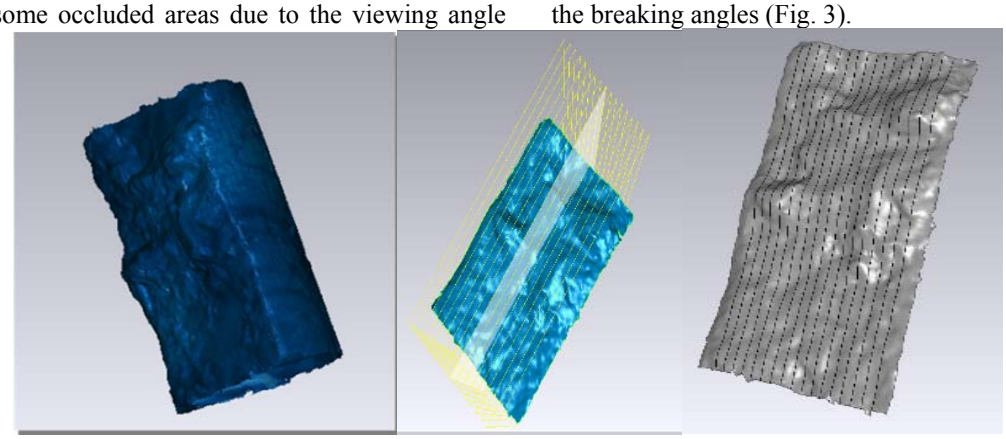

Figure 3. Surface Model and Produced Cross-Sections.

MATLAB Curve Fitting Toolbox was used to evaluate the data gathered from point cloud. MATLAB Curve Fitting Toolbox library provides optimized solver parameters and initial conditions (Exponential, Fourier series, Gaussian, Polynomials and Power series, etc.) to improve the quality of fitting. It also supports non-parametric modelling techniques, such as splines, interpolation, and smoothing. By the visual inspection of the fitted splines with different methods, it was decided that the usage of shape preserving interpolation method provided the best presentation of the geometry. Since its derivative gives the slope and the inverse of the slope is the roughness angle values; the first derivatives were calculated along the horizontal axis of curves. The starting point was taken on the South to North direction, and roughness angles were determined as seen in the Figure 3b, and they were divided into 2 directions for each profile.

Roughness angles were assumed to be in the "+" direction where all roughness angles looked towards the North and in the "-" direction where all roughness angles looked towards the South as shown in Figure 4.

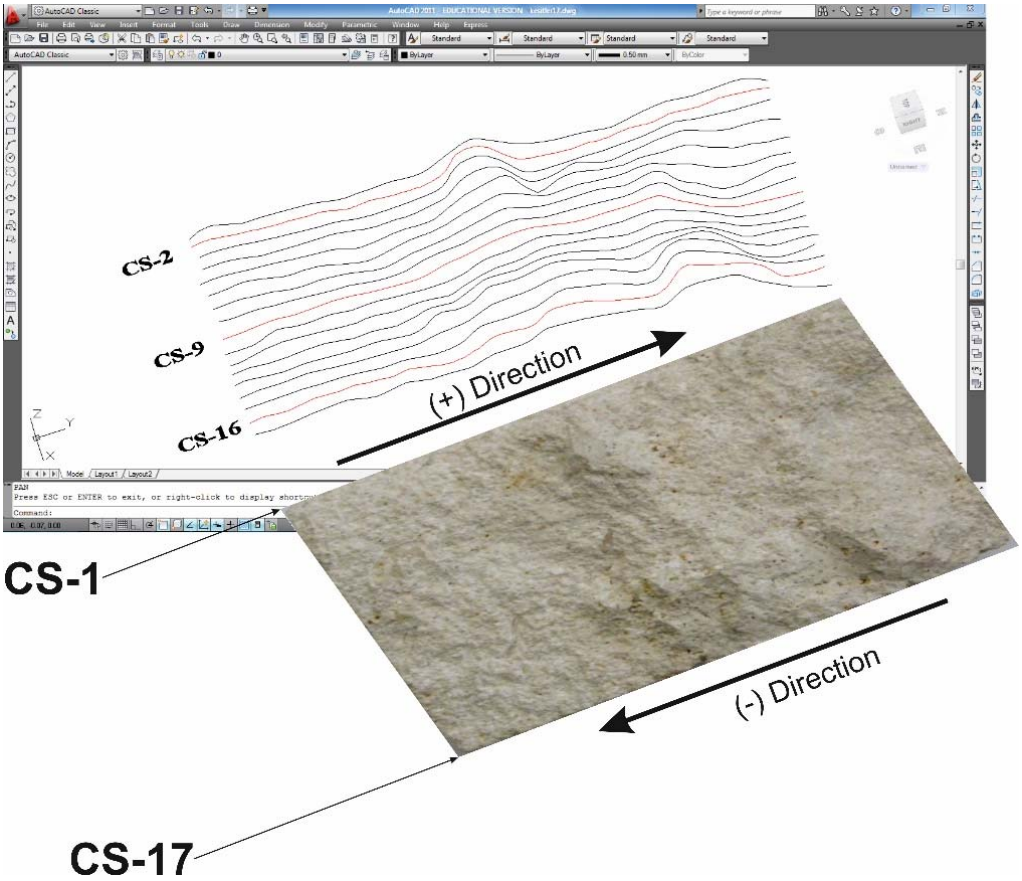

Figure 4. Rock Surface and Produced Cross-Sections

The total number of the roughness angle measurement points for the 17 profiles is 169578. 100616 points (54.34%) of the total measurements were calculated in the "-" direction and rest are in the "+" direction. Number of points and the lengths of profiles are given in Table 1. The maximum, minimum and average roughness angles in both the negative and positive directions are given in Table 2 for all profiles. After analyzing the roughness angles for "-" and "+" directions, the roughness angle numbers were determined following the successive two integer roughness angle values. These numbers and theirs percentages in both directions, and whole rock specimen surfaces are given in Table 3. The measured profiles of the surface and their polynomial equations according to minimum standard deviation rule are calculated and three of them are given in Table 4.

Table 1. Cross-Sections and Number of Points.

Cross- Section	Profile Length (mm)	Number of Points		
		(-) Direction	(+) Direction	Total
1	69.3	6909	3092	10001
2	69.2	5933	4067	10000
3	68.6	5551	4450	10001
4	69.9	6054	3947	10001
5	69.6	6515	3486	10001
6	69.3	5637	4364	10001
7	69.2	5893	3963	9856
8	68.7	6288	3713	10001
9	68.6	5670	4330	10000
10	69.5	6064	3937	10001
11	68.7	5713	4287	10000
12	68.8	5768	3943	9711
13	68.9	6566	3435	10001
14	68.2	5203	4798	10001
15	68.6	5241	4760	10001
16	68.5	5819	4181	10000
17	69.0	5792	4209	10001

Table 2. Profiles and minimum, average, maximum roughness angles.

Cross Section	(-) Direction Values			(+) Direction Values		
	Minimum	Maximum	Average Value	Minimum	Maximum	Average Value
1	0.00057	53.76746	10.24966	0.00678	57.44093	13.97666
2	0.00017	58.09700	10.92225	0.00133	59.32415	9.81189
3	0.00026	59.51028	13.99453	0.00234	50.15401	11.75792
4	0.00079	63.44434	14.27691	0.01061	39.87980	13.60156
5	0.00004	53.20169	15.00914	0.00076	30.56198	12.61094
6	0.00244	48.94721	15.56506	0.00663	22.05385	10.29962
7	0.00002	65.58133	13.42382	0.00019	22.13315	10.59833
8	0.00045	53.62265	11.88525	0.00231	19.49687	8.96328
9	0.00720	48.96845	12.81814	0.00077	21.58132	7.78613
10	0.00232	40.50336	12.66222	0.00000	32.64834	10.22719
11	0.00311	38.28470	14.01129	0.00165	25.76140	9.82412
12	0.00458	48.36064	13.57318	0.00268	36.54299	10.12892
13	0.00002	52.76161	13.98669	0.00051	46.59729	13.85158
14	0.00190	55.80606	17.05369	0.00057	44.82725	12.76530
15	0.00570	58.69937	17.44440	0.00009	55.50682	12.53443
16	0.00134	48.63212	16.35495	0.00118	55.08712	14.35045
17	0.00394	59.20337	14.85585	0.00269	47.87393	13.80740
Geometric Mean Value	0.00071	52.87508	13.86988	0.00096	36.72473	11.41006

Table 3 Roughness angle numbers and their percentage distribution on surface.

Roughness Angle Values	Roughness Angle Number (-) Direction	(-) Direction, (%)	Roughness Angle Number (+) Direction	(+) Direction, (%)	Surface Roughness Angle Number	Surface (%)
65 – 66	22	0.0219	0	0	22	0.0130
64 – 65	13	0.0129	0	0	13	0.0077
63 – 64	59	0.0586	0	0	59	0.0348
62 – 63	52	0.0517	0	0	52	0.0307
61 – 62	48	0.0477	0	0	48	0.0283
60 – 61	49	0.0487	0	0	49	0.0289
59 – 60	95	0.0944	21	0.0305	116	0.0684
58 – 59	152	0.1511	21	0.0305	173	0.1020
57 – 58	172	0.1709	36	0.0522	208	0.1227
56 – 57	128	0.1272	29	0.0421	157	0.0926
55 – 56	206	0.2047	89	0.1291	295	0.1740
54 – 55	132	0.1312	118	0.1711	250	0.1474
53 – 54	263	0.2614	100	0.1450	363	0.2141
52 – 53	357	0.3548	102	0.1479	459	0.2707
51 – 52	427	0.4244	70	0.1015	497	0.2931
50 – 51	272	0.2703	90	0.1305	362	0.2135
49 – 50	220	0.2187	103	0.1494	323	0.1905
48 – 49	471	0.4681	90	0.1305	561	0.3308
47 – 48	412	0.4095	133	0.1929	545	0.3214
46 – 47	355	0.3528	151	0.2190	506	0.2984
45 – 46	350	0.3479	148	0.2146	498	0.2937
44 – 45	353	0.3508	226	0.3277	579	0.3414
43 – 44	396	0.3936	173	0.2509	569	0.3355
42 – 43	324	0.3220	115	0.1668	439	0.2589
41 – 42	323	0.3210	157	0.2277	480	0.2831
40 – 41	475	0.4721	176	0.2552	651	0.3839
39 – 40	610	0.6063	179	0.2596	789	0.4653
38 – 39	495	0.4920	182	0.2639	677	0.3992
37 – 38	617	0.6132	161	0.2335	778	0.4588
36 – 37	626	0.6222	208	0.3016	834	0.4918
35 – 36	745	0.7404	234	0.3393	979	0.5773
34 – 35	996	0.9899	183	0.2654	1179	0.6953
33 – 34	816	0.8110	423	0.6134	1239	0.7306
32 – 33	618	0.6142	421	0.6105	1039	0.6127
31 – 32	920	0.9144	511	0.7410	1431	0.8439
30 – 31	783	0.7782	633	0.9179	1416	0.8350
29 – 30	741	0.7365	519	0.7526	1260	0.7430
28 – 29	955	0.9492	474	0.6873	1429	0.8427
27 – 28	1437	1.4282	470	0.6815	1907	1.1246
26 – 27	1144	1.1370	421	0.6105	1565	0.9229
25 – 26	1095	1.0883	503	0.7294	1598	0.9423
24 – 25	962	0.9561	621	0.9005	1583	0.9335
23 – 24	1104	1.0972	571	0.8280	1675	0.9877
22 – 23	1311	1.3030	603	0.8744	1914	1.1287
21 – 22	1509	1.4998	1088	1.5777	2597	1.5314
20 – 21	1233	1.2255	991	1.4370	2224	1.3115
19 – 20	1410	1.4014	1017	1.4747	2427	1.4312
18 – 19	1587	1.5773	1455	2.1099	3042	1.7939
17 – 18	2056	2.0434	1654	2.3984	3710	2.1878

16 – 17	2477	2.4618	1733	2.5130	4210	2.4826
15 – 16	2285	2.2710	2005	2.9074	4290	2.5298
14 – 15	2399	2.3843	1801	2.6116	4200	2.4767
13 – 14	2663	2.6467	1863	2.7015	4526	2.6690
12 – 13	2732	2.7153	2277	3.3018	5009	2.9538
11 – 12	3096	3.0770	2383	3.4555	5479	3.2310
10 – 11	3091	3.0721	2730	3.9587	5821	3.4326
9 – 10	3089	3.0701	2561	3.7136	5650	3.3318
8 – 9	4349	4.3224	2644	3.8340	6993	4.1238
7 – 8	4747	4.7179	3184	4.6170	7931	4.6769
6 – 7	4804	4.7746	4270	6.1918	9074	5.3509
5 – 6	4647	4.6185	3635	5.2710	8282	4.8839
4 – 5	4854	4.8243	3512	5.0927	8366	4.9334
3 – 4	4831	4.8014	3432	4.9767	8263	4.8727
2 – 3	5914	5.8778	3899	5.6538	9813	5.7867
1 – 2	6869	6.8269	4675	6.7791	11544	6.8075
0 – 1	7873	7.8248	6688	9.6981	14561	8.5866

Table 4. Original profiles (red) and profiles expressed by polynomial equations (blue).

Cross-Section 1

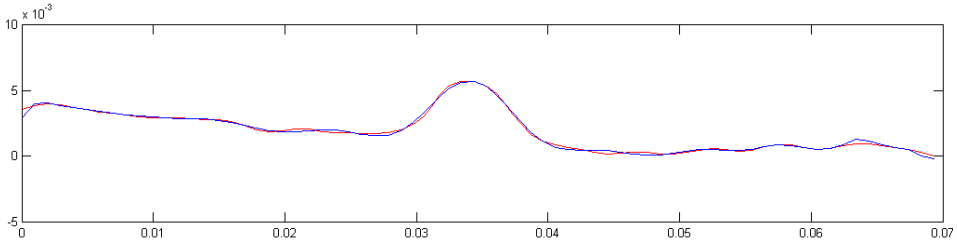

$y = -1.52\,e{+}45 * x^{30} + 9.73\,e{+}44 * x^{29} - 2.71\,e{+}44 * x^{28} + 4.21\,e{+}43 * x^{27} - 3.88\,e{+}42 * x^{26} + 2.07\,e{+}41 * x^{25} - 7.91\,e{+}39 * x^{24} + 8.61\,e{+}38 * x^{23} - 1.24\,e{+}38 * x^{22} + 1.02\,e{+}37 * x^{21} - 5.00\,e{+}35 * x^{20} + 2.05\,e{+}34 * x^{19} - 1.72\,e{+}33 * x^{18} + 1.79\,e{+}32 * x^{17} - 1.32\,e{+}31 * x^{16} + 6.74\,e{+}29 * x^{15} - 2.46\,e{+}28 * x^{14} + 6.49\,e{+}26 * x^{13} - 1.22\,e{+}25 * x^{12} + 1.51\,e{+}23 * x^{11} - 8.48\,e{+}20 * x^{10} - 8.63\,e{+}18 * x^{9} + 2.58\,e{+}17 * x^{8} - 3.01\,e{+}15 * x^{7} + 2.09\,e{+}13 * x^{6} - 8.65\,e{+}10 * x^{5} + 1.75\,e{+}08 * x^{4} + 7.72\,e{+}04 * x^{3} - 1.21\,e{+}03 * x^{2} + 2.15 * x + 2.88\,e{-}03$

Cross-Section 9

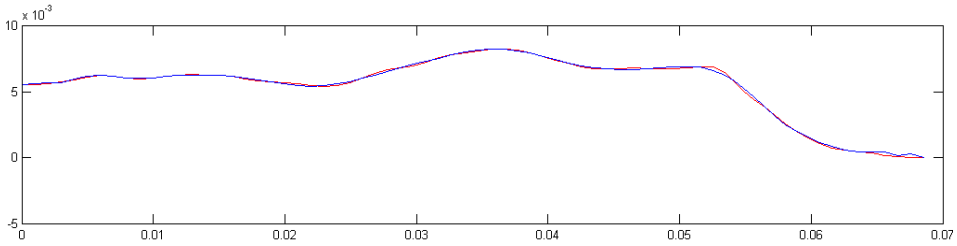

$y = -1.26\,e{+}37 * x^{24} + 8.69\,e{+}36 * x^{23} - 2.68\,e{+}36 * x^{22} + 4.77\,e{+}35 * x^{21} - 5.08\,e{+}34 * x^{20} + 2.53\,e{+}33 * x^{19} + 1.38\,e{+}32 * x^{18} - 4.05\,e{+}31 * x^{17} + 4.35\,e{+}30 * x^{16} - 3.09\,e{+}29 * x^{15} + 1.63\,e{+}28 * x^{14} - 6.59\,e{+}26 * x^{13} + 2.10\,e{+}25 * x^{12} - 5.26\,e{+}23 * x^{11} + 1.04\,e{+}22 * x^{10} - 1.61\,e{+}20 * x^{9} + 1.94\,e{+}18 * x^{8} - 1.77\,e{+}16 * x^{7} + 1.19\,e{+}14 * x^{6} - 5.68\,e{+}11 * x^{5} + 1.82\,e{+}09 * x^{4} - 3.56\,e{+}06 * x^{3} + 3.73\,e{+}03 * x^{2} - 1.48 * x + 5.56\,e{-}03$

Cross-Section 17

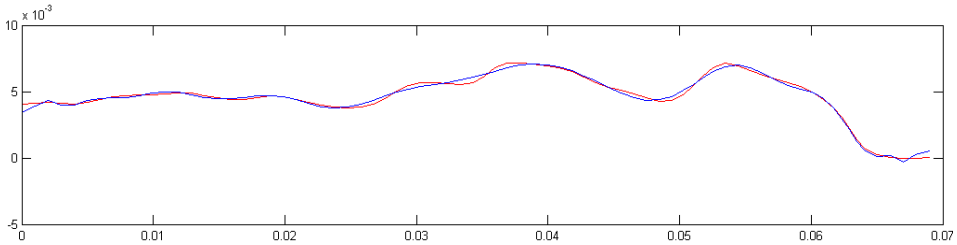

$y = -5.07\,e{+}37 * x^{24} + 3.82\,e{+}37 * x^{23} - 1.33\,e{+}37 * x^{22} + 2.85\,e{+}36 * x^{21} - 4.13\,e{+}35 * x^{20} + 4.28\,e{+}34 * x^{19} - 3.22\,e{+}33 * x^{18} + 1.71\,e{+}32 * x^{17} - 5.66\,e{+}30 * x^{16} + 3.01\,e{+}28 * x^{15} + 9.28\,e{+}27 * x^{14} - 6.61\,e{+}26 * x^{13} + 2.75\,e{+}25 * x^{12} - 8.13\,e{+}23 * x^{11} + 1.80\,e{+}22 * x^{10} - 3.04\,e{+}20 * x^{9} + 3.90\,e{+}18 * x^{8} - 3.76\,e{+}16 * x^{7} + 2.66\,e{+}14 * x^{6} - 1.33\,e{+}12 * x^{5} + 4.50\,e{+}09 * x^{4} - 9.36\,e{+}06 * x^{3} + 1.02\,e{+}04 * x^{2} - 3.62 * x + 3.40\,e{-}03$

Estimation of the Number of Roughness Angles

The number of roughness angles that lie in the two successive integers were analysed with the data given in Table 3. The limitation of the sample was that medium weight was chosen and it was close to the lower value for the porosity properties according to Anon (1979) classification, and all the results given below is valid for similar kind of limestone's in general. Data was analysed for the 17 sections separately along the both directions as shown in Fig. 3.

The values in the data set were scattered around 250 of roughness angles. Moreover, the number of calculated roughness angles between the two successive integer angles with the obtained equations also gave negative values for smaller roughness angle, which was physically impossible. Due to this fact, the data for the 17 profiles were evaluated together, and it was assumed to be representative of the specimen surfaces. The analysis resulted as a useful equation for the number of roughness angle values (NRAV) as given in Fig. 5. This relation is expressed by Equation 1 (r = 0.964) for "-" direction roughness angle measurements.

$$N_{RAV} = 7318.3 \times \exp^{(-0.0725 \times RAV)} \quad (1)$$

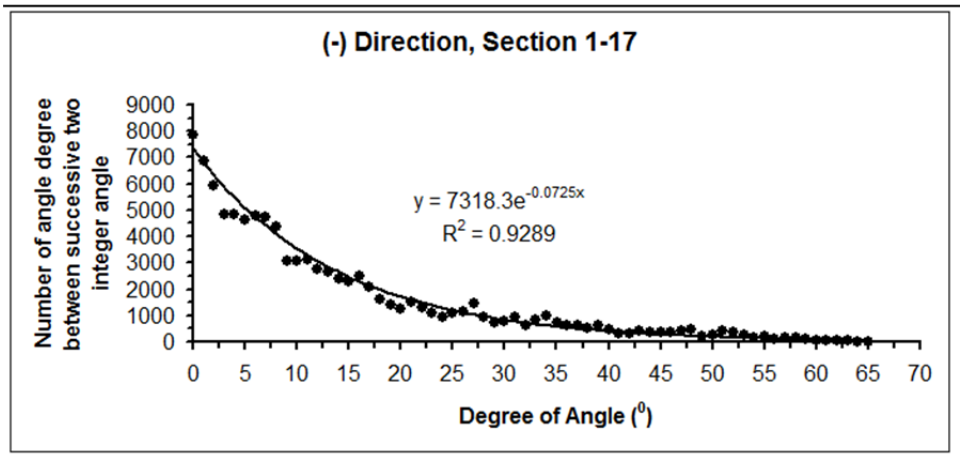

Figure 5. The mathematical relationship between roughness angle and number of roughness angle in two successive integers.

Users can calculate for percentage values of both the number of roughness angles and calculated values using Equation 1. Numerical values are quite proximate to the measured values as shown in Fig. 6. Furthermore, the relationship between the percentage values of both the number of roughness angles with the two successive integer angle values (PNRAV) and the roughness angle value (RAV) can be expressed by Equation 2 (r = 1) below for "-" direction roughness angle measurements.

$$PN_{RAV} = 7.2735 \times \exp^{(-0.0725 \times RAV)} \quad (2)$$

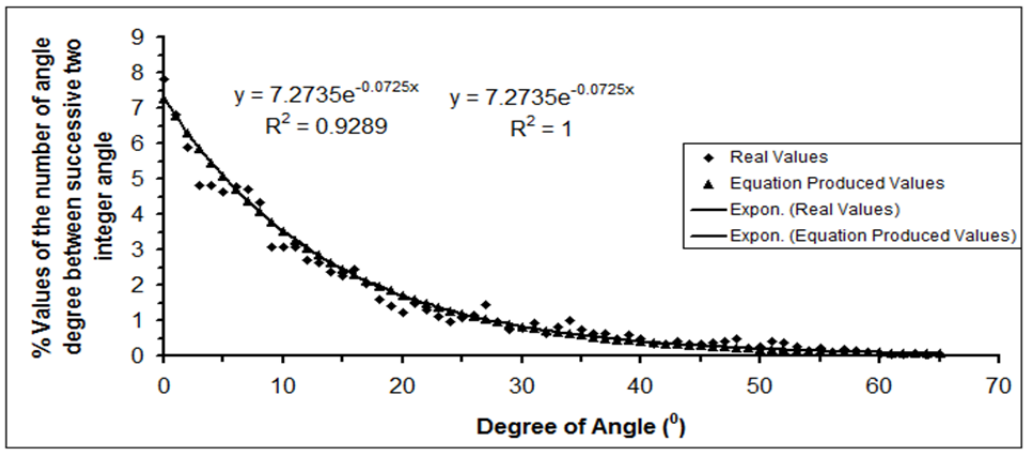

Figure 6. The mathematical relationship between roughness angle degree and the percentage of the number of roughness angles along the "-" direction.

It is possible to calculate the percentage values of smooth to stepped parts of the Class 2 limestone using Equation 2. According to this equation, the percentage of the number of roughness angles between 0 and 1 degree is 6.765% and, between 65 and 66 degree is 0.065%. These values decrease until 900. For example, they become 0.045%, 0.022% and 0.011% for 690 – 700, 790 – 800 and 890 – 900 roughness angles, respectively.

The same analyses were conducted for the "+" direction roughness angle measurements. The

number of roughness angle between the two successive integer roughness angles has been scattered. After the analysis; some negative values for the number of roughness angles were calculated for profile 2 and 16. Thus, the evaluation of all profile values together for the rock surface performed well and it gave a useful equation for the number of roughness angles (NRAV) for two successive integer roughness angles (RAV) for "+" direction roughness angle measurements. The analysed data is given in Fig. 7 and the proposed equation is given with Equation 3, where r = 0.982.

$$N_{RAV} = 5524.5 \times \exp^{(-0.0846 \times RAV)} \quad (3)$$

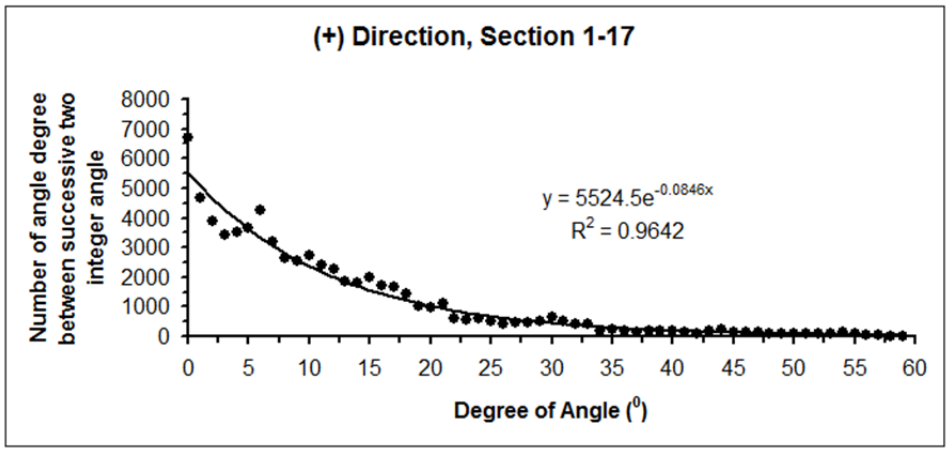

Figure 7. The mathematical relationship between roughness angle degree and roughness angle value numbers in two successive integers.

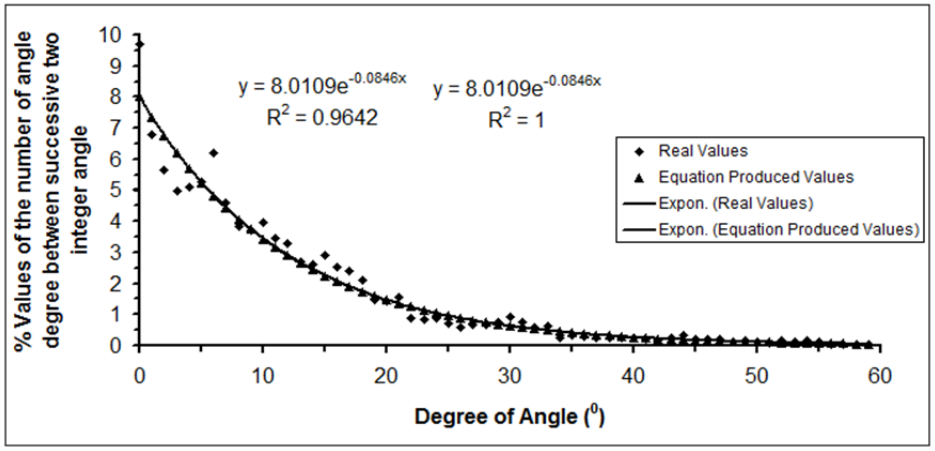

Figure 8. The mathematical relationship between roughness angle degree and the percentage of number of roughness angles in two successive integer roughness angles along the "-" direction.

The percentage values of both the number of roughness angles between the two successive integer angles and calculated values obtained from Equation 3 were also quite close to each other as shown in Fig. 8. The relationship between the percentage values of both the number of roughness angles with the two successive integer angle values (PNRAV) and the roughness angle value (RAV) can be expressed with Equation 4 (r = 1) below for "+" direction roughness angle measurements.

$$PN_{RAV} = 8.0109 \times \exp^{(-0.0846 \times RAV)} \quad (4)$$

Calculation of the percentage values of smooth and stepped parts of Class 2 limestone can also be possible by using Equation 3. According to Equation 3, the percentage of the number of roughness angles between 0 and 1 degree is 7.361% and, between 59 and 60 degree is 0.054%. This percentage values decrease until 900. For example, it becomes 0.023%, 0.010% and 0.004% for 690 – 700, 790 – 800 and 890 – 900 roughness angles, respectively.

In this part of the study, Class 2 limestone surface roughness was attempted to be analytically modelled for forecasting the number of roughness angle values (NRAV) between two successive integer roughness angle values (RAV) in nature. Equation 1 and 3 were used for forecasting the number of roughness angle values (NRAV) between two successive integer roughness angle values (RAV) in nature. The roughness angle is measured along the sliding direction; therefore, condition of the roughness profiles in nature, which is given in Fig. 8, determined whether to use Equation 1 or 3 for this purpose. Moreover, the percentage values of the number of roughness angles (NRAV) between two successive integer roughness angle values (RAV) in nature are forecasted by using Equation 2 or 4 for the rock surface along the "-" or "+" direction as shown in Fig. 9.

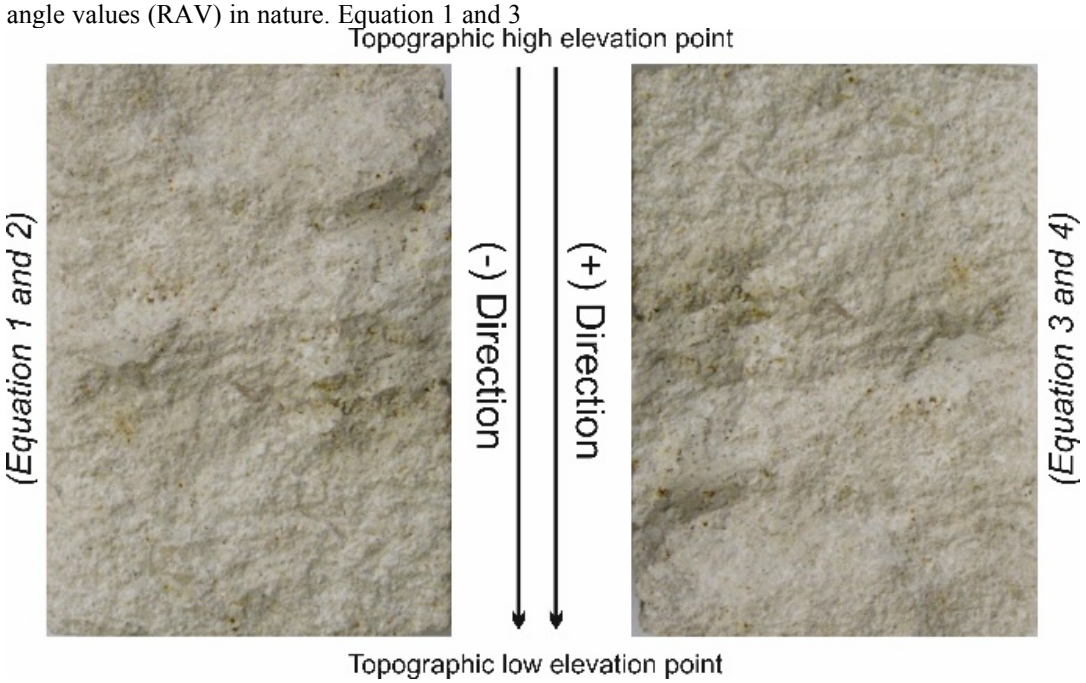

Figure 9. The condition of the rock surface either in the "-" or "+" direction in nature with related equations.

Results

Calculating the Minimum, Maximum and Average Roughness Angles of a Limestone Rock Surface

The following equations with the equation number of 5a and 5b were proposed for minimum, average and maximum roughness angle values for a Class 2 limestone based on the data set given in Table 2. For this, data set is enumerated from minimum to maximum for minimum, average and maximum values of data set and the proposed equations are related with the profile number (PN). The minimum roughness angle value (MinRAV) along a surface(s) may be determined with a power equation as given in Equation 5a (where r = 0.982) for "-" direction and in Equation 5b (where r = 0.973) for "+" direction as shown in Fig. 10.

$$Min_{RAV} = \left(6 \times 10^{-6}\right) \times PN^{2.4493} \quad (5a)$$

$$Min_{RAV} = \left(1 \times 10^{-5}\right) \times PN^{2.3217} \quad (5b)$$

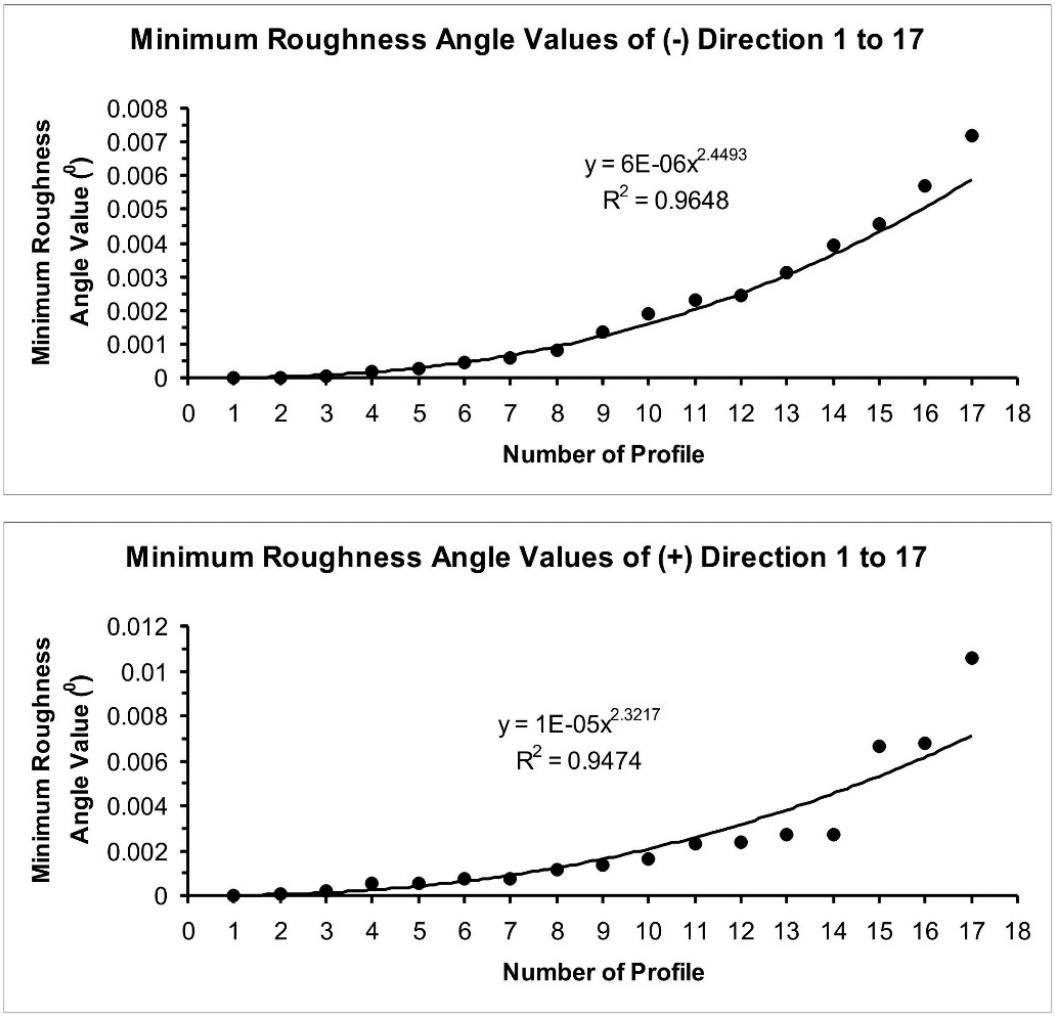

Figure 10. The mathematical relationship between roughness, profile number and minimum roughness angle.

Using equation 5a and 5b, the calculated roughness angle values are found different from the measured values between 0.38 and 2.37 times for the "-" direction and between 0.49 and 2.77 times for the "+" direction. Moreover, the geometric mean value is 0.00075 for the "-" direction and 0.00097 for the "+" direction which are the 1.05 and 1.01 times of the geometric mean value of the measured minimum roughness angles values given in Table 2, respectively. New equations were needed for calculating the geometric mean value of the measured minimum roughness angles values as given in Table 2. The relationship between the obtained roughness angle values (GRAV) using equations 5a and 5b and the measured values were investigated and results are shown in Fig. 11.

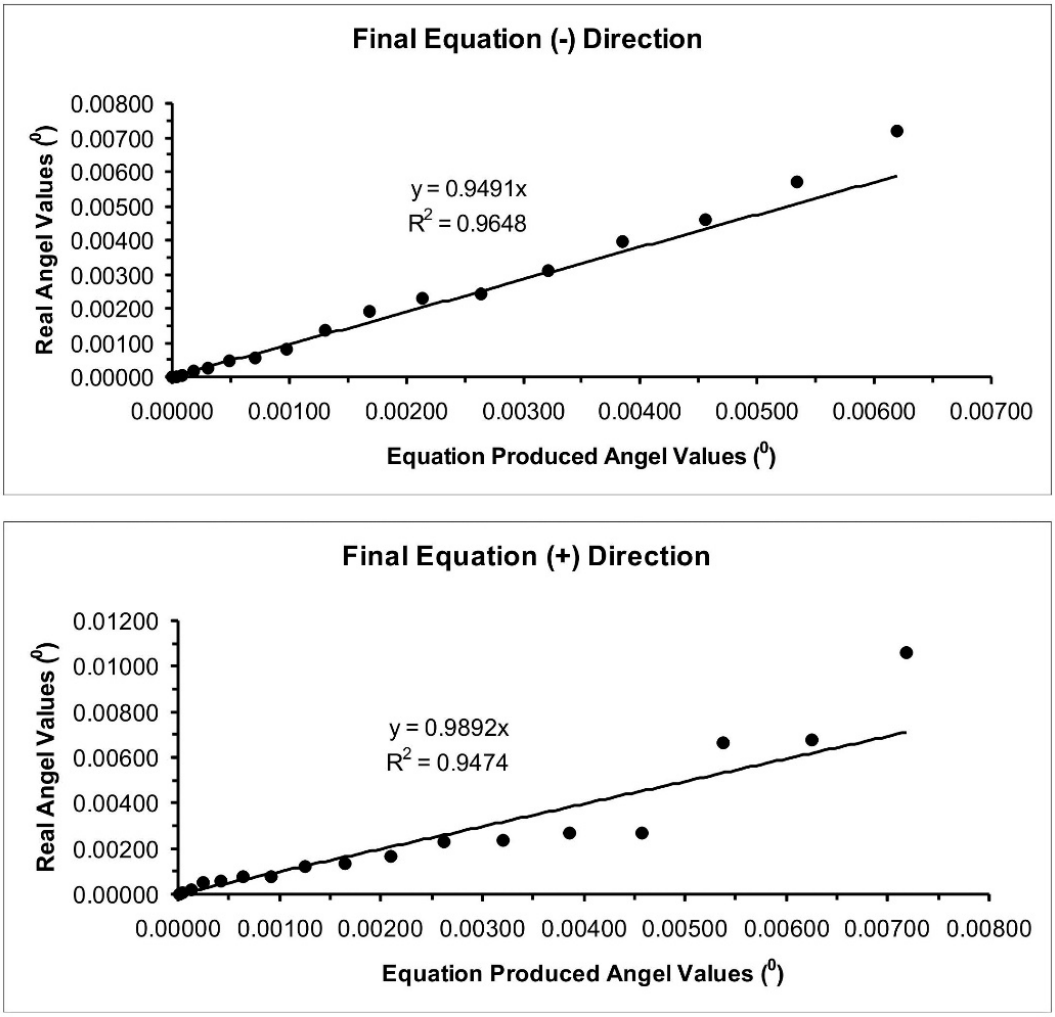

Figure 11. The mathematical relationship between gathered roughness angle values using Eq. 5a, b and the measured minimum roughness angle values.

Equation 6a (where r = 0.982) for "-" direction and Equation 6b (where r = 0.973) for "+" direction, are the final equations for forecasting the minimum roughness angle value (MinRAV) along a surface(s).

$$Min_{RAV} = 0.9491 \times G_{RAV} \quad (6a)$$

$$Min_{RAV} = 0.9892 \times G_{RAV} \quad (6b)$$

Equations 6a and 6b give the forecasted roughness angle values that differ from the measured values between 0.36 and 2.25 times for the "-" direction and between 0.48 and 2.74 times for the "+" direction. However, these equations give the geometric mean values of roughness surface with 100% similarity for the "-" and 99.99% similarity for the "+" directions for the values given in Table 2. In addition, Equations 6a and 6b show that the minimum roughness angle value of a surface may be measured as 0.37 and 0.48 times for a measured value for the "-" and "+" directions related with data cloud and also in nature as shown in Fig. 9. The same judgment is also possible for the highest minimum roughness angle of a surface obtained from profiles. In this case, the highest minimum roughness of a surface may be measured as 2.37 and 2.77 times from the measured value for "-" and "+" directions, respectively. Although the given values for the smallest and the highest minimum roughness

angle value of a surface obtained from roughness profiles mentioned above may be sufficient to solve the problem as these are based on the 17 roughness profiles. However, number of profiles can be increased by easily calculating using equation 6a and 6b. In this study, the roughness angle values were investigated in a core specimen with 6.94 cm x 4.95 cm dimensions indicating that the profile width is ~0.29 cm or the specimen is divided into 17 profiles. Equation 6a and 6b can be used if the higher accuracy is required more than the chosen profile width. If the profile number is chosen as 50, (~1:100 ratio are used with a 0.0994 cm. profile width) which is the highly sensitive evaluation for the studied surface, the highest minimum roughness angle value of a surface will be 0.082560 and 0.087050 for "-" and for "+" directions, respectively (Figure 9). Moreover, the same approach may be applied in nature (Fig. 9), and these equations can be used for calculating the average minimum roughness of a surface and the minimum values based on profile width will depend on the sensitivity of the engineering project.

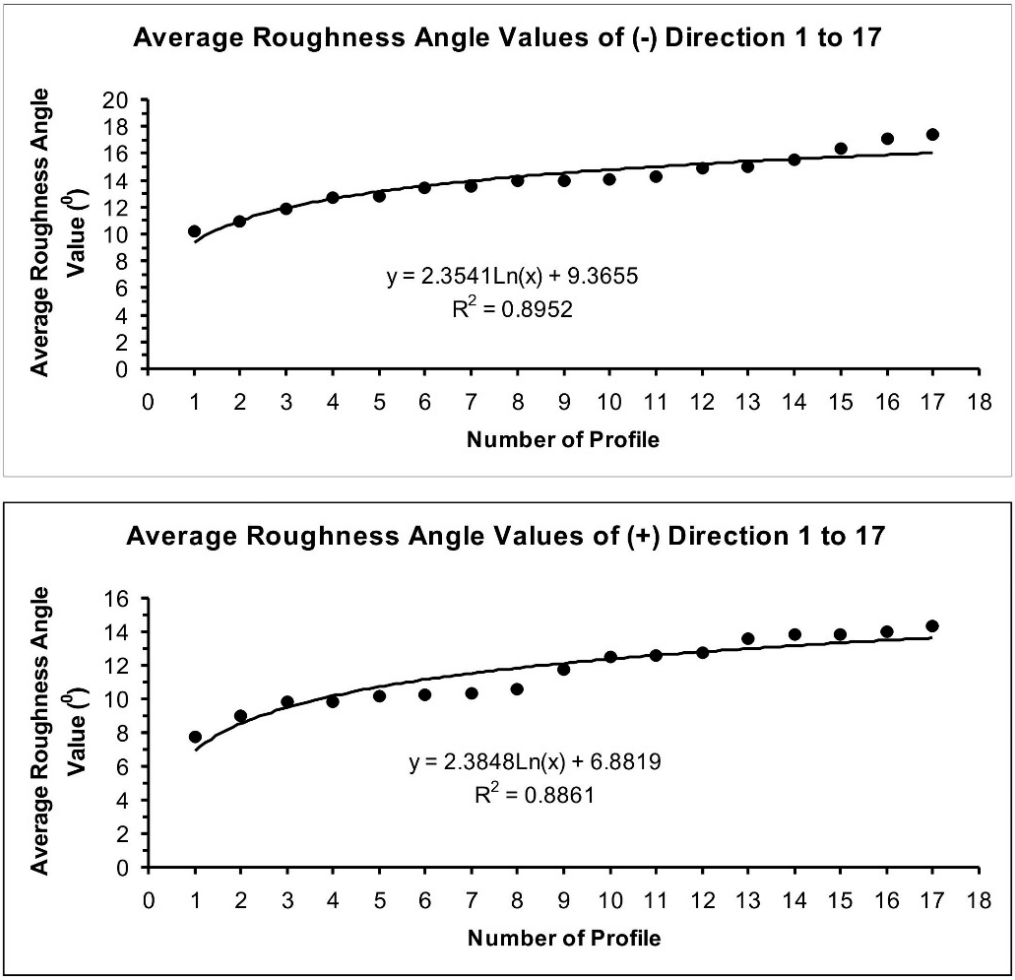

Figure 12. The mathematical relationship between roughness profile number and average roughness angle.

The same analyses were carried out for the average and maximum roughness angle values of a surface given in Fig. 9. The mathematical relationships between profile number (PN) and the average roughness angle values (AVGRAV) along a surface(s) are determined with a logarithmic equation. Equation 7a (where r = 0.946) for "-" direction and Equation 7b (where r = 0.941) for "+" direction as shown in Fig. 12.

$$AVG_{RAv} = 2.3541LN(PN) + 9.3655 \quad (7a)$$

$$AVG_{RAV} = 2.3848LN(PN) + 6.8819 \quad (7b)$$

The percentage of the geometric mean value obtained by Equation 7a and 7b is 100% of the geometric mean of the measured roughness angle values of all 17 profiles both for "-" and "+" directions. Thus, these equations make it possible to sufficiently evaluate the average roughness angle value of a Class 2 limestone surface. Moreover, the similarity of the average values calculated by Equation 7a and 7b among the measured roughness angle values average mean change between 0.91 and 1.06 times and, 0.88 and 1.12 times for "-" and "+" directions, respectively. If the profile number (PN) increases to 1:100 ratio for the studied core sample is the ~50 sections, the average roughness angle value of the surface is 18.570 and 16.210 for the "-" and "+" directions, respectively.

The mathematical relationship between profile number (PN) and the maximum roughness angle values (MaxRAV) along a surface(s) may also be determined with a logarithmic equation. Equation 8a (where r = 0.96) for the "-" direction and Equation 8b (where r = 0.917) for the "+" direction as shown in Fig. 13.

$$Max_{RAv} = 8.8387LN(PN) + 35.956 \quad (8a)$$

$$Max_{RAV} = 16.119LN(PN) + 7.4935 \quad (8b)$$

The percentage of the geometric mean value obtained by Equation 8a is 100% and for Equation 8b is 98.23% of the geometric mean of measured roughness angle values for the "-" and the "+" directions. However, the discrepancy between the forecasted and measured values are 0.93 and 1.06 times for the "-" and 0.38 and 1.35 times for the "+" directions. Hence, Equation 8a and 8b may be adequate for forecasting the average value of a maximum roughness angle in a Class 2 rock surface. However, Equation 8b will not be fully sufficient for the maximum roughness angle of a Class 2 rock surface obtained from profiles. In spite of this fact, Equation 8b can be used for forecasting the maximum roughness angle values for a Class 2 rock surfaces as shown in Fig 8. Hence, Equation 8b may be used as Equation 8a in order to determine the maximum value of the maximum roughness angel values. If the studied surface is divided into 50 profiles, the maximum roughness angle values are determined as 70.530 and 70.550 for the "-" and the "+" directions using proposed equations, respectively.

Results and Discussion

Roughness of a discontinuity has an important role on the shear strength of discontinuity. Determining the discontinuity of surface roughness and roughness angles both require experience and considerable equipment in conventional methods. Whereas, these methods need more attention and the sensitivity depends on the human capability. Therefore, methods that depend on gauge measurements such as optical, photogrammetric or laser based are more preferable. Advantages of the digital point cloud approach are the ability to characterize the rock surfaces precisely and the possibility to collect high amount of data to estimate rock surface roughness along desirable scale in a short time.

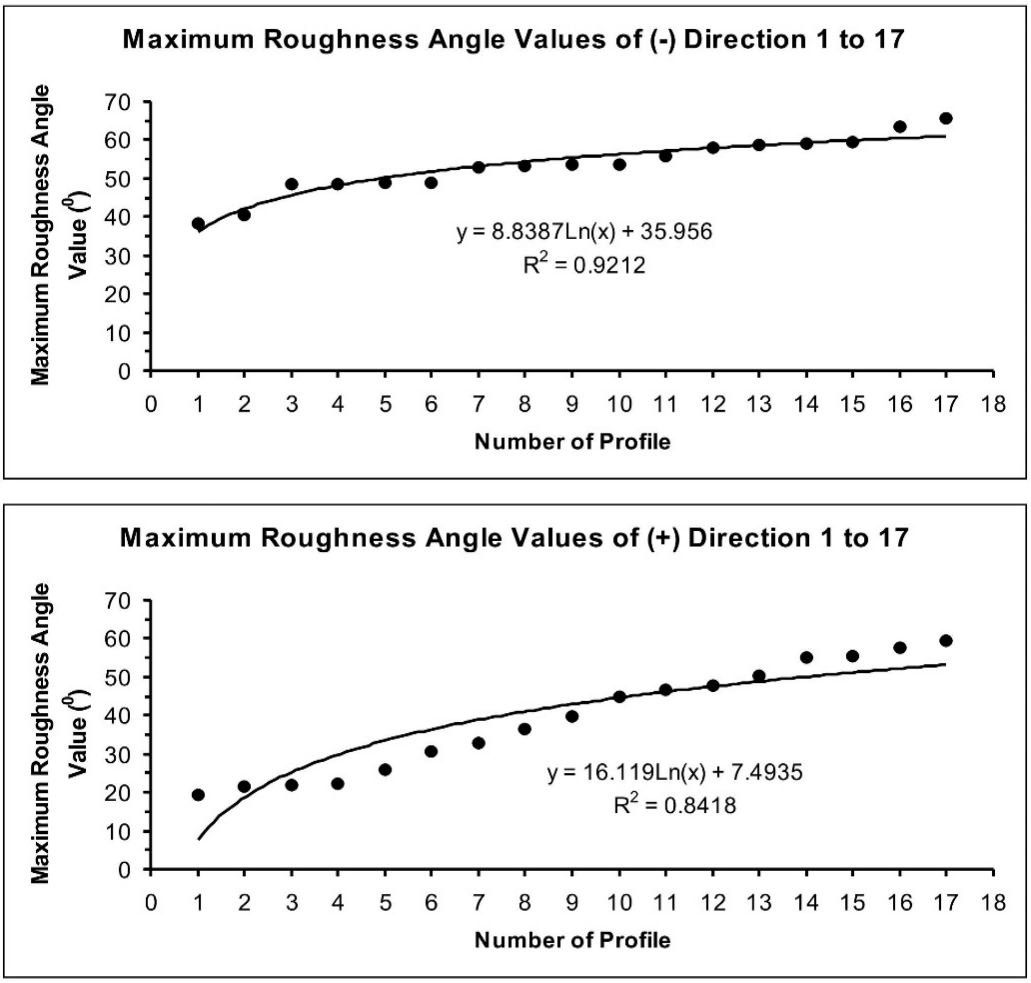

Figure 13. The mathematical relationship between the roughness profile number and the maximum roughness angle.

On the other hand, the disadvantages are the cost of the equipment and software and the time required to train inexperienced users, the need of accurate survey camera or laser scanner and the potential difficulty of extracting and analysing rock surface profiles in directions that differ from the point cloud coordinate axes. Recent technologies are the easiest way to provide fast and accurate data for creating 3D surface models from roughness measurements. These techniques are versatile and prolific for the users to measure roughness along any desired profile in different directions. These profiles can be obtained with the chosen resolution for the spatial span along the discontinuity surface. This study considers the roughness angle measurement by the use of 3D surface imaging method. Additionally, the surface is modelled from the spatial data so that the roughness angles are tangent to each profile. Each profile contains 2 different group of measurements; one with the "-" and the other with the "+" signs for opposite directions. These signs convey a mathematical meaning and present directions of the arctangents. Following the 3D modelling, the surface of the Class 2 limestone, which has 18% – 20% porosity values, the mathematical relations were studied with 169578 data points, ~54.34% of which (100616 points) is in the "-" direction and, ~45.66% of which (68962 points) is in the "+" direction.

The ratio of the percentage values along the "+" direction to the percentage values along the "-" direction is 0.84 which may show the

asymmetry of the surface roughness. This is also the evidence that there is a need for using the 3D laser scanner for determining roughness angles of a surface in roughness analysis. Analysing the data cloud showed that the maximum percentage scattering of the roughness angle following the two successive degrees, was about 10% between the 00 and 10. Using the proposed exponential equations (1 – 4) for Class 2 limestone which has 18% – 20% porosity values, forecasting the number of the roughness angle and its percentage between the two successive integer values will be easy. Moreover, the relationship between profile number and the minimum, average and maximum roughness angles of each profile (power equations) is useful for forecasting the average value of each profile's minimum values with full accuracy.

The similar relationship was performed for average and maximum values and some logarithmic equations were proposed for this purpose with 98.23% and 100% accuracy. Furthermore, by using these proposed equations, it will be possible both to forecast the minimum and maximum values of the minimum, average and maximum roughness angles of a surface, if more data cloud is taken than the evaluated points and if the surface model is divided into more roughness profiles (e.g. 1:100 ratios). In this way, the pre-evaluations for shearing, the choice of correct roughness angle values for viaduct, bridge or especially concrete dam projects will be possible by using these equations. If the same study is performed for other type rocks according to Anon classification, the obtained polynomial (or other types) equations will be useful in numerical modelling, and the proposed equations will be more easy to use in pre-evaluations of engineering project design.

References

Akça, D., Grün, A., Breuckmann, B. and Lahanier, C. (2007). High Definition 3D-Scanning of Arts Objects and Paintings, Optical 3D Measurement Techniques VIII, July 9-12, Zurich, Switzerland.

Anon, (1979). Classification of rocks and soils for engineering geological mapping. Part I– Rock and soil materials', Bull. Int. Ass. Engg Geol., 19, 364-371.

Aydar, U., Akyol, O., Duran, Z. (2011). A Low-Cost Laser Scanning System Design, XXIII CIPA Symposium, 12/16 September 2011, Prague, Czech Republic.

Barton, N. R. (1973). Review of a new shear strength criterion for rock joints. Eng. Geol., 8, 287-332.

Barton, N. R. and Choubey, V. (1977). The shear strength of rock joints in theory and practice. Rock Mechanics, 10, 1-54.

Fardin, N., Feng, Q. and Stephansson, O. (2004). Application of a new in situ 3D laser scanner to study the scale effect on the rock joint surface roughness. International Journal of Rock Mechanics and Mining Sciences, 41(2): 329-335.

Fecker, E. and Rengers, N. F. (1971). Measurement of large scale roughness of rock planes by means of profilograph and geological compass. 1st Int. Symp. Rock Mech, Nancy pp.1-18.

Galante, G., Piacentini, M. and Ruisi, V. F. (1991). Surface roughness detection by tool image processing, Wear, 148(2): 211-220.

Grasselli, G. and Egger, P. (2000). 3D surface characterization for the prediction of the shear strength of rocks joints. In: A. Aachen (Editor), Symposium EUROCK 2000, Germany, pp. 281-286.

Grima, M. A. (1994). Scale effect on shear strength behaviour of ISRM roughness profiles. MSc Thesis, ITC Delft, Kanaalweg 3, 2628 EB Deft, The Netherlands, 200p.

Harrison, J. P. and Rasouli, V. (2001). In-plane analysis of fracture surface roughness: anisotropy and scale effect in anisotropy. In: H.K. Tinucci JP, Elsworth D (Editor), Proceeding of the 38th US Rock Mechanics Symposium, Lisse, Netherlands, Swets & Zeitlinger Washington DC, USA, pp. 777-783.

Hong, E., Lee, I and Lee, J. (2006). Measurement of rock joint roughness by 3D scanner. Geotechnical Testing Journal, 29(6):8.

ISRM, (1978). Commission on standardization of laboratory and field test: Suggested methods for the quantitative description of discontinuities in rock masses. International Journal of Rock Mechanics and Mining

Sciences & Geomechanics Abstracts, 15(6): 319-368.

Jaeger, J. C. (1971). Frictions of rocks and stability of rock slope. Geotechnique, 21, 97-134.

Kerstiens, C. M. D. (1999). A generic UDEC model for rock joint shear test, including roughness characterization MSc Thesis, TU Delft, Kanaalweg 3, 2628 EB Delf, The Netherlands, 211p.

Maerz, N. H., Franklin, J. H. and Bennet, C. P. (1990). Joint roughness measurement using shadow profilometry. International Journal of Rock Mechanics and Mining Sciences & Geomechanics Abstracts, 27(5): 329-343.

Milne, D., Germain, P., Grant, D. and Noble, P. (1991). Field observation for the standardization of the NGI classification system for underground mine design. International Congress of Rock Mechanics, A.A, Balkema, Aachen, Germany.

Patton, F. D. (1966). Multiple modes of shear failure in rock. Proc. 1st. Congress, Int. Soc. Rock Mechanics, Lizbon, 1, 509-513.

Rahman, Z., Slob, S. and Hack, H. R. G. K. (2006). Deriving roughness characteristics of rock mass discontinuities from terrestrial laser scan data. Proc. Engineering Geology for tomorrow's cities. 10th IAEG Congress, Nottingham, United Kingdom, 6-10 Sept. 2006 (article, accepted for publication).

Weissbach, G. (1978). A new method for the determination of the roughness of rock joints in the laboratory. International Journal of Rock Mechanics and Mining Sciences & Geomechanics Abstracts, 15(3): 131-133.

Wickens, E. H. and Barton, N. R. (1971). Application of photogrammetry to the stability of excavated rock slopes. Photogrammetric Record, 7(37): 46-54.

Yılbaş, Z. and Hasmi, M. S. J. (1999). Surface roughness measurement using an optical system. Journal of Materials Processing Technology, 88(1-3): 10-22.

Zagorchev, L. and Goshtasby, A. (2006): A paintbrush lazer range scanner. Computer Vision and Image Understanding 101.